

Supporting Information

Selective Hydrodeoxygenation of Acetophenone Derivatives Using a $\text{Fe}_{25}\text{Ru}_{75}@\text{SILP}$ Catalyst: a Practical Approach to the Synthesis of Alkyl Phenols and Anilines

Lisa Goclik, Henrik Walschus, Alexis Bordet,* Walter Leitner*

Table of Contents

Safety Warning.....	2
1 General	2
2 Analytics.....	2
3 GC-Analysis	2
4 Synthesis of the $\text{Fe}_{25}\text{Ru}_{75}@\text{SILP}$ catalyst.....	3
4.1 Synthesis of 3-Iodopropyltriethoxysilane	3
4.2 Synthesis of [1-butyl-3-(3-triethoxysilylpropyl)imidazolium]iodide	3
4.3 Synthesis of [1-butyl-3-(3-triethoxysilylpropyl)imidazolium]NTf ₂	4
4.4 Synthesis of SILP	4
4.5 Synthesis of Ru(cod)(cot)	4
4.6 Synthesis of $\text{Fe}_{25}\text{Ru}_{75}@\text{SILP}$	5
5 Autoclave reactions.....	6
6 Isolation of Products	6
6.1 Isolation of long chain alkyl phenols	6
6.2 Isolation of alkyl anilines	6
7 Continuous flow reactions using the H-Cube.....	6
8 Supplementary figures and tables	8
9 Synthetic approach evaluation.....	10
10 NMR characterization associated to isolated products	13

Safety Warning

High pressure experiments with compressed H₂ must be carried out only with appropriate equipment and under rigorous safety precautions.

1 General

If not otherwise stated, the synthesis of the ionic liquids (ILs), the supported ionic liquid phases (SILPs) and the nanoparticles immobilized on SILPs (NPs@SILPs) were carried out under an inert atmosphere (Ar) using standard Schlenk techniques or inside a glovebox. All the synthesized materials were stored under inert atmosphere. All other chemicals and solvents were commercially available and used without further purification.

2 Analytics

All solution state NMR were recorded on a Bruker Ascend 400 spectrometer at room temperature. The coupling constants (*J*) are given in Hertz (Hz), and the chemical shifts (δ) are expressed in ppm, relative to TMS at 25 °C. Gas chromatography (GC) was performed on a Shimadzu GC-2030 equipped with a FID-detector and a CP-WAX-52CB column from Agilent. Gas chromatography coupled with a mass spectrometer (GC-MS) were performed on a Shimadzu QP2020.

BET measurements were performed on a Quadrasorb SI from Quantachrom Instruments.

Transmission and scanning transmission electron microscopy (TEM and STEM) were performed on a Hitachi HF2000 cold FEG operating at 200 kV at the Max-Planck-Institut für Kohlenforschung. Samples were prepared by depositing the powder onto a copper TEM grid with an amorphous carbon support film.

Scanning electron microscopy with energy dispersive X-ray spectroscopy (SEM/EDS) was performed on a Hitachi S-3500N operating at 30kV at the Max-Planck-Institut für Kohlenforschung. Samples were prepared by depositing the powder onto a tape and flattening it out to obtain an even surface for analysis. The metal ratios, loadings and standard deviations are average values obtained by measuring several (3) batches of each material.

3 GC-Analysis

The determination of the yields were done by gas chromatography with FID. For most of the reactions, the following conditions and equipment settings have been used:

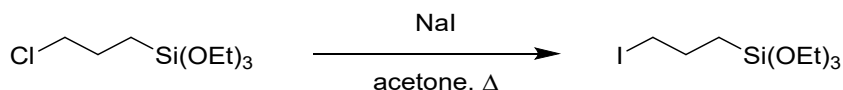
Stationary Phase (Column) from Agilent	RTX-1 (0.25 μ m, 0.25 mm, 30 m)
Mobile Phase (Carrier Gas)	1.9 mL·min ⁻¹ He
Flow Control Mode Linear Velocity	40.0 cm·sec ⁻¹

Injection Volume	0.3 μ L
Injector Temperature	250 $^{\circ}$ C
Split Ratio	35
Temperature Program	50 $^{\circ}$ C for 8 min, to 200 $^{\circ}$ C with 2 $^{\circ}$ C \cdot min $^{-1}$, 300 $^{\circ}$ C for 2 min
Detector Temperature	310 $^{\circ}$ C

The identification of the compounds was done by injecting the pure compounds in GC-FID, or by GC-MS.

4 Synthesis of the Fe₂₅Ru₇₅@SILP catalyst

4.1 Synthesis of 3-Iodopropyltriethoxysilane



Sodium iodide (1.05 eq., 436 mmol, 65.4 g) was dried *in vacuo* at 100 $^{\circ}$ C overnight. The dried sodium iodide was weighed inside a glovebox and dissolved in 250 mL acetone (extra dry, acroseal). 3-Chloropropylethoxysilane (1.00 eq., 415 mmol, 100 mL) was added via cannulisation. The mixture was refluxed (100 $^{\circ}$ C) and stirred under argon atmosphere for 72 h.

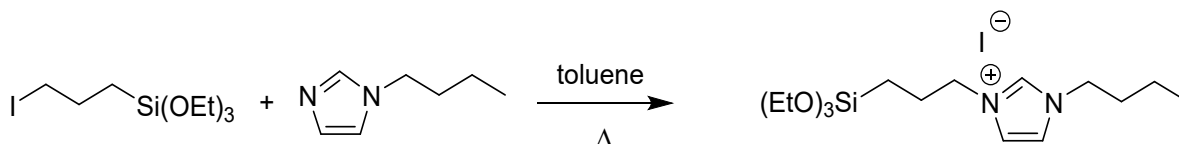
The reaction mixture was allowed to cool down and the acetone was evaporated *in vacuo* (additional cooling trap between flask and Schlenk line). The product was purified by distillation (4.0 x 10⁻² mbar, 100 $^{\circ}$ C, head temperature: 78 $^{\circ}$ C). The product was yielded as an orange liquid (126.3 g, 380 mmol, 87%).

NMR:

¹H NMR (400 MHz, Chloroform-*d*) δ (ppm) = 3.78 (q, *J* = 7.0 Hz, 6H), 3.18 (t, *J* = 7.0 Hz, 2H), 1.95 – 1.84 (m, 2H), 1.19 (t, *J* = 7.0 Hz, 9H), 0.75 – 0.62 (m, 2H).

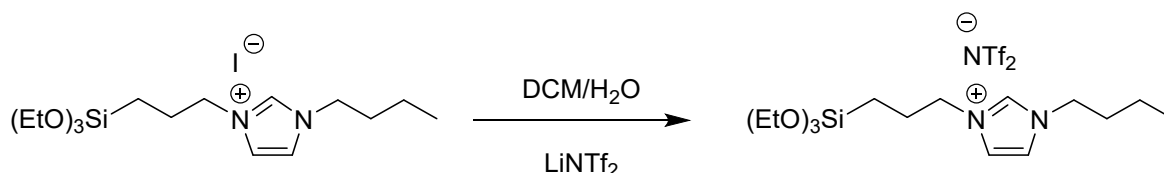
¹³C NMR (100 MHz, Chloroform-*d*) δ (ppm) = 58.47 (3C), 27.56 (1C), 18.30 (3C), 12.25 (1C), 10.76 (1C).

4.2 Synthesis of [1-butyl-3-(3-triethoxysilylpropyl)imidazolium]iodide



N-butylimidazole (1.3 eq., 30.5 mmol, 3.769 g, 4.0 mL) was dried over molecular sieves 3 \AA overnight and added to 3-Iodopropyltriethoxysilane (1 eq., 29.7 mmol, 9.880 g, 7.6 mL). The mixture was diluted in toluene (50 mL) and stirred under reflux (130 $^{\circ}$ C) and argon for 72 h. The toluene was removed with a syringe and [1-butyl-3-(3-triethoxysilylpropyl)imidazolium]iodide (IL) was washed with toluene (1 x 20 mL) and pentane (1 x 20 mL). The IL was dried *in vacuo* and yielded as a yellow liquid (10.3 g, 22.5 mmol, 76%).

4.3 Synthesis of [1-butyl-3-(3-triethoxysilylpropyl)imidazolium]NTf₂



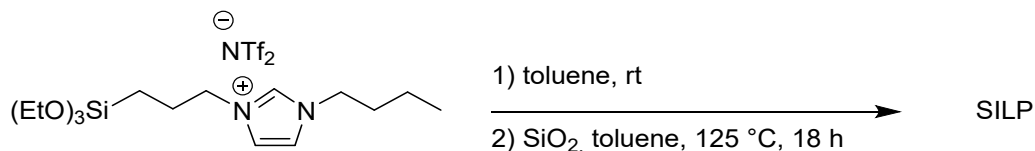
[1-butyl-3-(3-triethoxysilylpropyl)imidazolium]iodide was dissolved in DCM (50 mL). LiNTf₂ (8.326 g) was dissolved in 25 mL dest. H₂O and added to the DCM-phase. The mixture was stirred for 60 min at rt. The H₂O phase was separated and the organic phase was washed with dest. H₂O (3 x 20 mL). The DCM was removed *in vacuo*. [1-butyl-3-(3-triethoxysilylpropyl)imidazolium]NTf₂ was dried *in vacuo* at 50 °C overnight and yielded as a yellow liquid.

NMR:

¹H NMR (400 MHz, Chloroform-*d*) δ (ppm) = 8.82 (s, 1H), 7.35 – 7.25 (m, 2H), 4.17 (q, J = 7.1 Hz, 4H), 3.78 (q, J = 7.0 Hz, 6H), 2.03 – 1.88 (m, 2H), 1.82 (p, J = 7.6 Hz, 2H), 1.33 (dq, J = 14.8, 7.4 Hz, 2H), 1.18 (t, J = 7.0 Hz, 9H), 0.92 (t, J = 7.4 Hz, 3H), 0.61 – 0.47 (m, 2H).

¹³C NMR (100 MHz, Chloroform-*d*) δ (ppm) = 122.23 (1C), 121.46 (1C), 118.29 (1C), 58.63 (1C), 51.90 (1C), 49.97 (1C), 32.00 (1C), 24.28 (1C), 19.35 (1C), 18.23 (1C), 13.24 (1C), 6.95 (1C).

4.4 Synthesis of SILP



[1-butyl-3-(triethoxysilylpropyl)imidazolium]NTf₂ (5.4 g, 8.8 mmol) was weighed into a Schlenk flask inside a glovebox and stirred in dry toluene (20 mL) at r.t. until complete dissolution (~ 1 h). SiO₂ (10.0 g, dehydroxylated at 500 °C) was weighed into another Schlenk flask and suspended in dry toluene (50 mL). The ionic liquid solution was added to the SiO₂ suspension and stirred with a magnetic stir bar under reflux (125 °C).

After 18 h the reaction mixture was allowed to cool down and the toluene was decanted through a filter. The filter solution was kept to determine the unbound IL. The SILP was washed with DCM (3 x 20 mL) and dried *in vacuo* at 60 °C overnight. The washing solutions were united with the filter solution and the solvents were removed.

4.5 Synthesis of Ru(cod)(cot)

Into a three neck round bottom flask, equipped with a cooler (with Ar-valve), an Ar-valve and a plug, RuCl₃·3 H₂O (1 g, 3.8 mmol) was introduced under argon. The plug was replaced by a septum and Ethanol (20

mL, dry and degassed) was added. After 2 min of slow stirring, cyclooctadiene (30 mL, 326.1 mmol, distilled and filtered through alumina) was added and the resulting mixture was stirred for 2 min again. The septum was removed and Zink dust (9 g) was added with a funnel. The flask was closed and the reaction mixture was stirred for exactly 3 h at 80 °C (time is starting from the beginning of the heating). After 3 h, the reaction mixture was allowed to cool down. A filtration over celite (which was heated overnight in the oven at 120 °C and left on a frit under argon for 3 hours) was carried out under argon atmosphere. The residue in the flask was washed out with 2 x 20 mL dry benzene and filtered as well through the frit. By evaporation of the benzene in *vacuo* (extra cooling trap installed), a brown highly viscous liquid was obtained. A second frit with 7 cm alumina (which was heated overnight in the oven at 120 °C left on a frit under argon for 3 hours) was prepared before. This alumina was wetted with 30 mL pentane. The brown residue was extracted with dry pentane (3x 30 mL). The solution was filtered quickly through the frit, which must not run dry at any point of the filtration process. More pentane (~ 120 mL) was used to flush the frit and filter the solution through it. Once the filtrate became colourless, the filtration was finished and the solution concentrated under vacuum to approximately 15 mL. The flask was stored in the freezer overnight. The next day, it was cooled down to -78 °C (dry ice/acetone) to form yellow-orange crystals (crystallization may last longer than one day). The precipitate was transferred to a schlenk tube and stored in the freezer and the crystals were dried in *vacuo* (252 mg, 0.8 mmol, 21%). If the NMR in deuterated benzene shows some impurities, the crystals can be dissolved in pentane, filtered through a syringe filter and recrystallized.

^1H NMR (400 MHz, Benzene- d_6) δ (ppm) = 5.30 (dd, J = 5.1, 2.2 Hz, 2H), 4.87 – 4.73 (m, 2H), 3.87 (d, J = 11.0 Hz, 2H), 3.03 (s, 4H), 2.36 (s, 8H), 1.78 (ddt, J = 12.6, 10.6, 5.3 Hz, 2H), 1.03 – 0.83 (m, 2H).

^{13}C NMR (100 MHz, Benzene- d_6) δ (ppm) = 101.05 (10 C), 99.00 (6C).

4.6 Synthesis of $\text{Fe}_{25}\text{Ru}_{75}@\text{SILP}$

A solution of $\{\text{Fe}[\text{N}(\text{Si}(\text{CH}_3)_3)_2]_2\}_2$ (18.0 mg, 0.05 mmol Fe) in mesitylene (2 mL) was combined with a solution of $[\text{Ru}(\text{cod})(\text{cot})]$ (47.0 mg, 0.15 mmol Ru) in mesitylene (2 mL) in a Fischer-Porter bottle (70 mL). The SILP (500 mg) was added to the solution of the metal precursors along with mesitylene (1 mL) and the reaction mixture was stirred under argon at room temperature for 30 min. The Fischer-Porter bottle was evacuated and backfilled with H_2 and the suspension was stirred under H_2 (3 bar) at 150 °C for 18 h. Under this reducing environment a black powder was obtained indicating the immobilization of the NPs onto the SILP. Mesitylene was decanted and $\text{Fe}_{25}\text{Ru}_{75}@\text{SILP}$ were washed with fresh toluene (3 x 3 mL) and dried *in vacuo* at rt for 1 h.

$\text{Fe}_{40}\text{Ru}_{60}@\text{SILP}$ and $\text{Fe}_{60}\text{Ru}_{40}@\text{SILP}$ were prepared following the same protocol with adapted quantities of Fe and Ru precursors.

5 Autoclave reactions

The substrate (25 eq., 0.1 mmol), catalyst (10 mg, containing 0.004 mmol metal) and solvent (mesitylene, 0.5 mL) were weighed inside of a glovebox into the autoclave. The autoclave was closed, transferred out of the glovebox and pressurized with 50 bar hydrogen. After heating the autoclave under stirring (500 rpm) to 175 °C for 16 h, it was cooled down in a water bath and depressurized. The GC samples were prepared by adding acetone (250 mg) to the reaction mixture and taking a sample through a syringe with a filter. To the sample, decane (internal standard, 20 mg) and acetone (200 mg) were added. For all amines, methanol/dioxane (1/1) was used as solvent for the GC samples.

6 Isolation of Products

6.1 Isolation of long chain alkyl phenols

The isolation of the long chain alkylphenols was carried out by adding 300 mg acetone to the reaction mixture and filtering through a syringe filter. By evaporating the solvent, the pure products were yielded. In the following, the structures, yields and NMR data of the products are reported.

6.2 Isolation of alkyl anilines

The isolation of the products from the hydrodeoxygenation of amino and nitroacetophenones was carried out by filtration of the reaction mixture through a short silica column in order to separate the mesitylene and the catalyst from the product. The products were then yielded by evaporation of the solvent. In the following, the structures, yields and NMR data of the products are reported.

7 Continuous flow reactions using the H-Cube

The continuous flow experiments were carried out using an H-Cube Pro equipped with a Phoenix reactor from ThalesNano (Figure S5).



Figure S1: H-Cube Pro equipped with a Phoenix reactor from ThalesNano.

The reactor (Catcart, 70 mm) was filled with the catalyst (~ 450 mg) inside of the glovebox and sealed. The sealing was pressed inside of the metal part by using the Catcart press. The Catcart was stored under argon atmosphere until it was installed in the H-Cube. The substrate solution (0.025 mol·L⁻¹ in a dry and degassed solvent such as anisole or mesitylene) was kept under argon and degassed by bubbling argon through it.

While using the H-Cube, the substrate solution as well as the washing solvent were kept under an argon flow. The H-Cube was washed with the pure solvent at 3 mL·min⁻¹ for ca. 10 min. The CatCart was placed into the flow reactor. Prior to catalysis, the catalyst was heated at 175°C under a flow of anisole (1 mL·min⁻¹) and H₂ (50 bar; gas flow rate under standard conditions = 90 NmL·min⁻¹) until the conditions reached a stable mode. The substrate solution was introduced into the system (0.015 mol·L⁻¹ 3',5'-dimethoxy-4'-hydroxyacetophenone (**20**) in anisole or 0.015 mol·L⁻¹ 4'-hydroxynonanophneone (**7**) in mesitylene) with a flow of 0.5 mL·min⁻¹. The reaction time starts at this point. Samples were drawn to measure the conversion and yield by GC measurements.

For the substrate switch, the H-Cube was started as described above. After the reaction interval with the first substrate (45 min) was carried out, a washing period (30 min, 2 mL·min⁻¹) was started. For the first washing anisole was used, in the following periods, heptane was used after reaction with 3',5'-dimethoxy-4'-hydroxyacetophenone (**20**) and mesitylene was used after reaction with 4'-hydroxynonanophneone (**7**). The substrate bottle was exchanged and the next reaction period was started by switching back to "reactant" and decreasing the flow to 0.5 mL·min⁻¹.

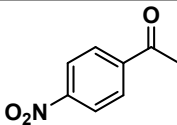
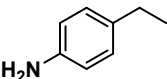
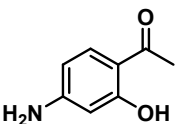
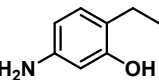
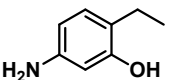
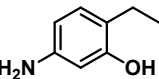
8 Supplementary figures and tables

Table S1: Characterization of the Fe₂₅Ru₇₅@SILP catalyst based on TEM, SEM/EDS and BET measurements before and after stability test in continuous flow.

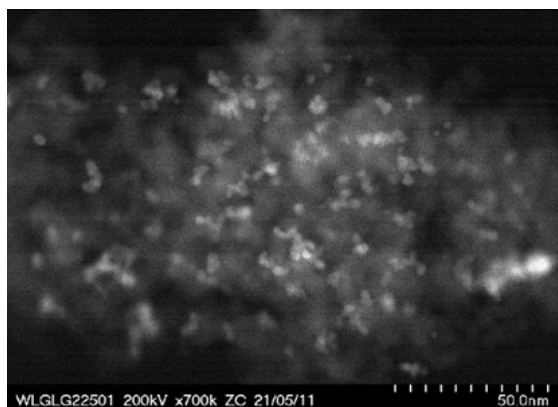
Catalyst	Surface area (m ² ·g ⁻¹)	NP size (nm)	Metal loading (mmol·g ⁻¹)	Metal ratio ^[a] (%)	
				Fe	Ru
Fe ₁₀₀ @SILP ^[5]	n.d.	3.3 ± 0.5	0.371	99 ± 1	1 ± 1
Fe ₆₀ Ru ₄₀ @SILP ^[5]	n.d.	3.2 ± 0.5	0.407	61 ± 4	39 ± 4
Fe ₄₀ Ru ₆₀ @SILP ^[5]	n.d.	2.8 ± 0.4	0.401	42 ± 3	58 ± 3
Fe ₂₅ Ru ₇₅ @SILP	240.7	3.3 ± 0.6	0.403	23 ± 5	77 ± 5
Fe ₂₅ Ru ₇₅ @SILP <i>after catalysis</i>	232.1	3.1 ± 0.6	0.395	29 ± 5	71 ± 5
Ru ₁₀₀ @SILP ^[5]	n.d.	3.6 ± 0.7	0.369	1 ± 1	99 ± 1

NPs sizes were determined by TEM. Metal ratio and loading were determined using SEM/EDS (Fe-K / Ru-L). ^[a] The average values and standard deviations were determined through the characterization of several batches (typically 3) of each material.

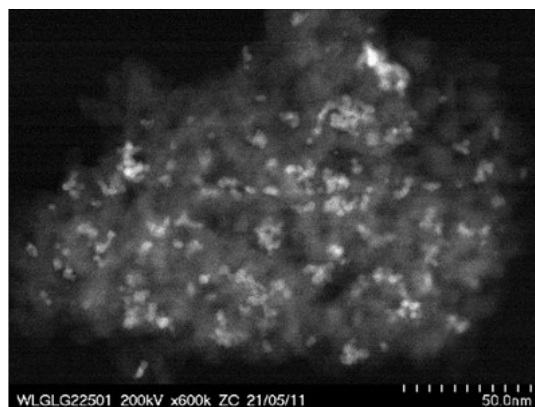
Table S2: Selective hydrodeoxygenation of model compounds in anisole.

Entry	substrate	product	X [%]	Y [%] ^[a]
1	 1	 1c	>99	94
2	 12	 12c	>99	99
3	 8	 8c	>99	96

Conditions: Catalyst: Fe₂₅Ru₇₅@SILP (10 mg), 0.5 mL solvent (anisole), 50 bar H₂, 175 °C, 16 h, 500 rpm. Product yields determined by GD-FID using decane as internal standard; ^[a] by-products: dimers



particle size: 3.3 (\pm 0.6) nm



particle size: 3.1 (\pm 0.6) nm

Figure S2: TEM images of the Fe₂₅Ru₇₅@SILP catalyst before (left) and after the catalysis (right) in continuous flow stability test.

For the optimization of the reaction conditions, the system was started under the listed conditions (Table S4). The reaction conditions were kept for 90 min. A sample for GC analysis was taken every 30 min.

Table S3: Optimization of the reaction conditions for the substrate switch in continuous flow.

Entry	Solvent	Substrate	T [°C]	P H ₂ [bar]	Substrate [mol·L ⁻¹]	X [%]	Y _c [%]
1	anisole	7	175	50	0.025	65	10
2	anisole	7	190	50	0.025	80	30
3	anisole	7	200	50	0.025	80	40
4	anisole	7	175	70	0.025	30-60	0-13
5	anisole	7	90	70	0.025	60	18
6	anisole	7	200	70	0.025	40	12
7	mesitylene	7	175	50	0.025	98	75
8	mesitylene	7	175	50	0.015	>99	95
9	anisole	20	175	50	0.025	98	68
10	anisole	20	175	50	0.015	>99	95

Conditions: 60 NmL·min⁻¹ H₂ flow, 0.5 ml·min⁻¹ substrate flow, substrate solutions: 3',5'-dimethoxy-4'-hydroxyacetophenone in anisole and 4'-hydroxynonanophneone in mesitylene, residence time: 18 s, Fe₂₅Ru₇₅@SILP (478.7 mg, 0.182 mmol metal). Product yields determined by GD-FID using decane as internal standard. X = conversion, Y = yield, **xc** = **7c** or **20c**.

9 Synthetic approach evaluation

The hydrodeoxygenation-based synthetic approach we propose in this study was systematically compared to conventional methods for the preparation of 2'-hydroxy-4-ethylaniline (**12**) and 4'-nonylphenol (**8**), the two products highlighted in Figure 1b-c. The Friedel-Crafts acylation step to produce acetophenone derivatives was included in the evaluation. The detailed synthetic routes are shown in Figure S1-S4.

Five parameters related to the green chemistry principles were taken into consideration to rank the pathways, *i.e.* the overall reaction yield (*Y*), the atom economy (*AE*), the number of steps (*Steps*), the hazardous nature of the reagents (*Safety*), and the economical aspect (difference of value between the product and the starting substrate, *Eco*).

The *AE* was calculated as follows:

$$AE = \frac{\text{total molecular weight of desired product}}{\text{total molecular weight of all reactants}} \cdot 100$$

The *Safety* parameter was evaluated qualitatively by ranking the different pathways based on the hazardous nature of the reactants that they involve. For that, a scale of one to five was used (one = most hazardous, 5 = least hazardous) as shown in Table S1. For example the average safety ranking for the classical synthesis pathway of 2-hydroxy-4-ethylanilin is determined as follows: $\text{Safety} = (1+1+4+1)/4 = 1.75 \approx 2$.

The parameter *Eco* represents here the different of price between the starting materials and the desired products (\Rightarrow how high is the addition of value). In both cases, our approach provides a better difference and the *Eco* is set arbitrarily to 5. For the conventional pathways, the addition of value is still attractive, and *Eco* was thus set to 4.

Parameters *Y* and *Steps* are self-explaining and quantitative.

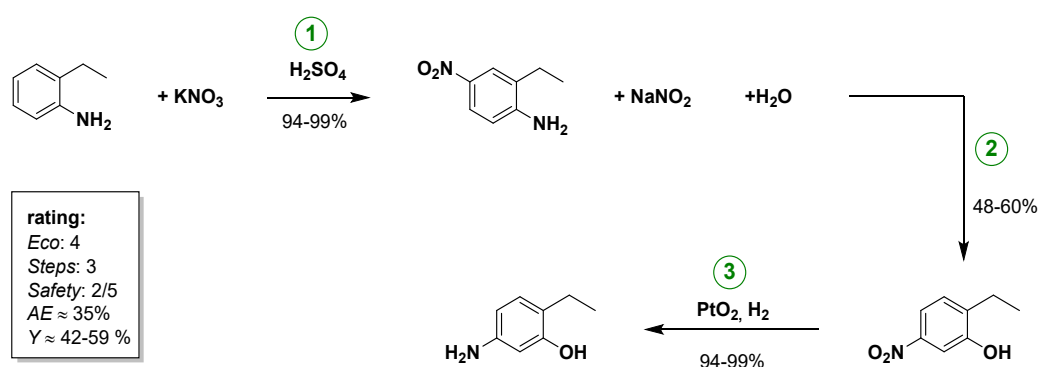


Figure S3: Conventional synthesis pathway for 2-hydroxy-4-ethylanilin (**12**).¹

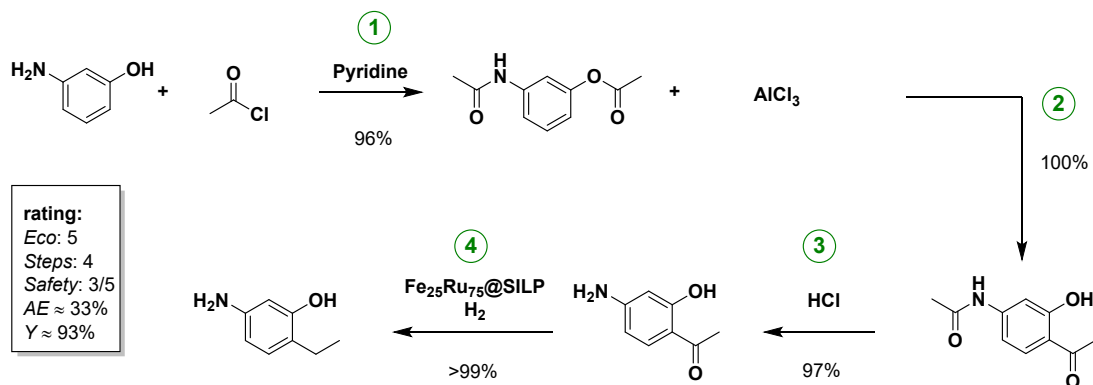


Figure S4: Our synthesis pathway for 2-hydroxy-4-ethylanilin (**12**).²

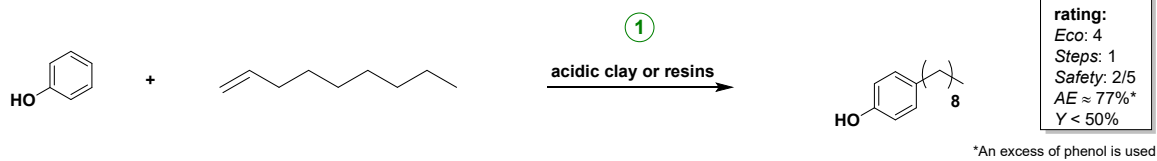


Figure S5: Conventional synthesis pathway for 4-n-nonylphenol (**8**).³

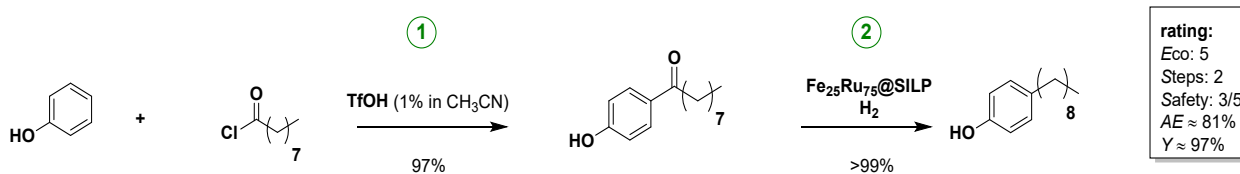


Figure S6: Our synthesis pathway for 4-n-nonylphenol (**8**).⁴

Table S4: Rating of the reactants.

GHS ranking	
1	explosive, oxidizing, toxic, health hazard
2	harmful, flammable, environmental, corrosive (combination of 3 hazards)
3	harmful, flammable, environmental, corrosive (combination of 2 hazards)
4	harmful, flammable, environmental, corrosive (1 hazard)
5	-

Chemical	CAS	Mw (g/mol)	Price (euros/g)	GHS Hazard
2-ethylaniline	578-54-1	109.1	0.32	toxic + harmful
KNO ₃	7757-79-1	101.1	0.09	oxidizing + harmful
H ₂ SO ₄	7664-93-9	98.8	-	corrosive
NaNO ₂	7632-00-0	69	0.12	oxidizing + toxic + environmental
3-aminophenole	591-27-5	109.1	0.15	harmful + environmental
acetylchloride	75-36-5	78.5	0.11	Flammable + harmful + corrosive
pyridine	110-86-1	79.1	-	harmful + flammable
AlCl ₃	7446-70-0	133.3	-	corrosive
HCl	7647-01-0	36.5	-	harmful + corrosive
5-amino-2-ethylphenol	207923-07-7	137.18	871.60	Product
phenol	108-95-2	94.1	0.046	hazardous + toxic + environmental
nonene	124-11-8	126.2	7.92	harmful + flammable
phenol	108-95-2	94.1	0.046	hazardous + toxic + environmental
nonanoyl chloride	764-85-2	176.7	1.4	corrosive
nonylphenol	84852-15-3	220.4	47.90	Product

10 NMR characterization associated to isolated products

4'-ethylphenol (1c)

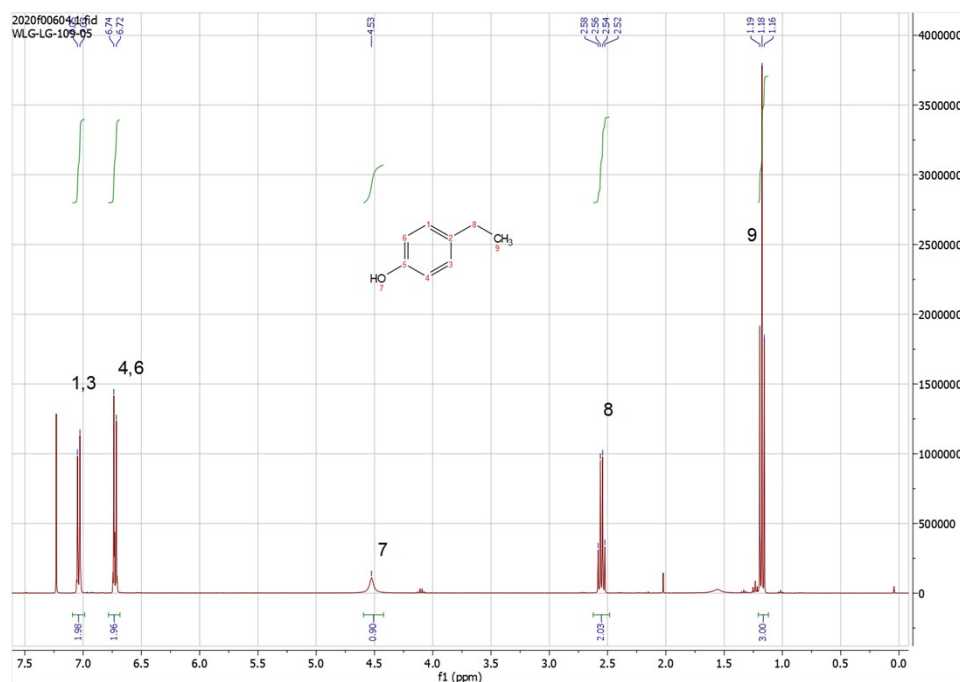


Figure S7: ¹H NMR of 4'-ethylphenol.

¹H NMR (400 MHz, Chloroform-*d*) δ (ppm) = 7.04 (d, J = 8.6 Hz, 2H), 6.73 (d, J = 8.6 Hz, 2H), 4.53 (s, 1H), 2.55 (q, J = 7.6 Hz, 2H), 1.18 (t, J = 7.6 Hz, 3H).

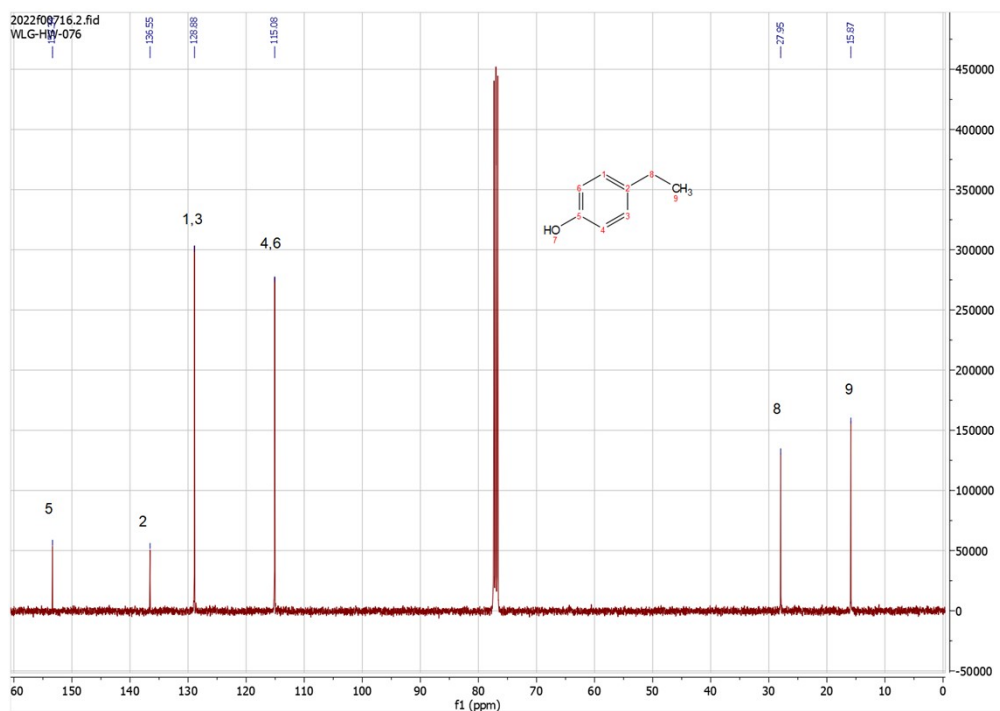


Figure S8: ¹³C NMR of 4'-ethylphenol.

¹³C{¹H} NMR (100 MHz, Chloroform-*d*) δ (ppm) = 153.34 (1C), 136.55 (1C), 128.88 (2C), 115.08 (2C), 27.95 (1C), 15.87 (1C).

4'-butylphenol (2c)

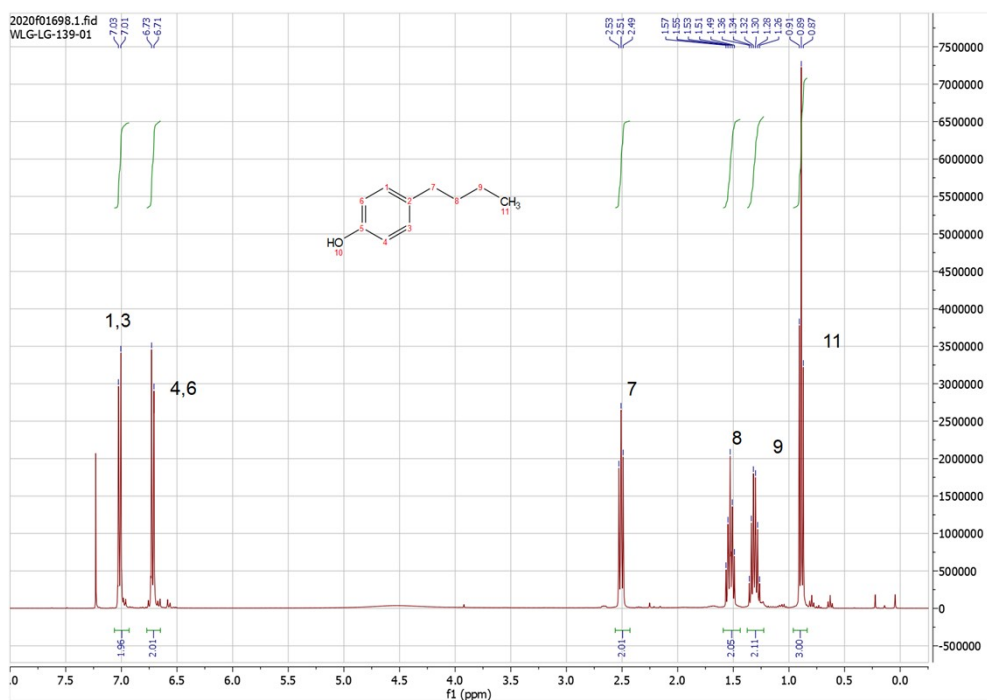


Figure S9: ^1H NMR of 4'-butylphenol.

^1H NMR (400 MHz, Chloroform-*d*) δ (ppm) = 7.02 (d, J = 8.5 Hz, 2H), 6.72 (d, J = 8.4 Hz, 2H), 2.53 – 2.49 (t, 2H), 1.53 (p, J = 7.5 Hz, 2H), 1.31 (dq, J = 14.7, 7.3 Hz, 2H), 0.89 (t, J = 7.3 Hz, 3H).

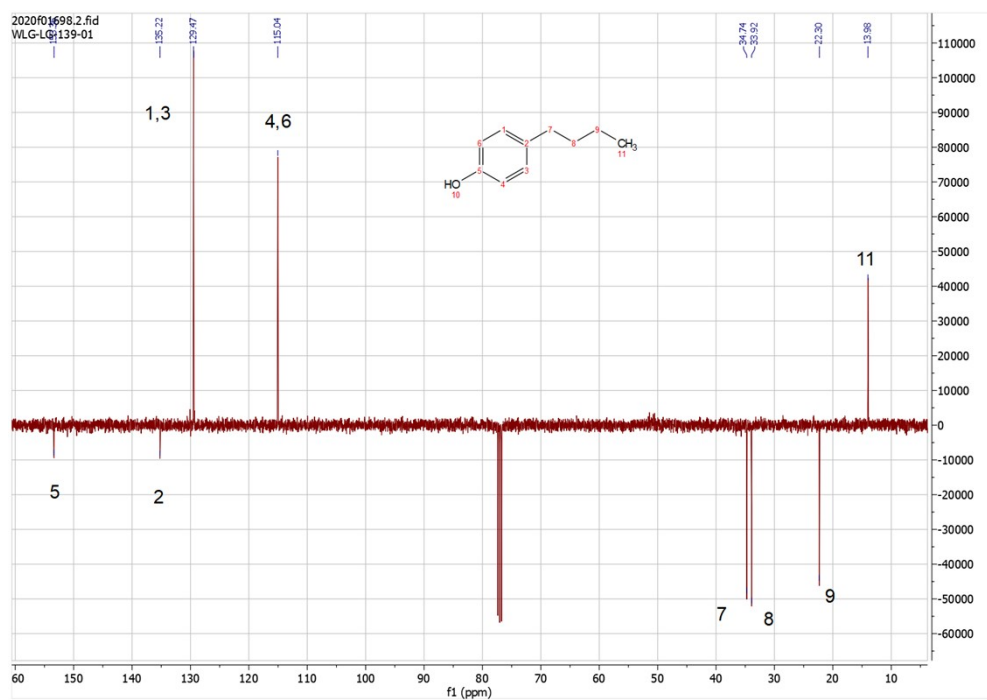


Figure S10: ^{13}C NMR of 4'-butylphenol.

^{13}C (APT) NMR (100 MHz, Chloroform-*d*) δ (ppm) = 153.36 (1C), 135.22 (1C), 129.47 (2C), 115.04 (2C), 34.74 (1C), 33.92 (1C), 22.30 (1C), 13.98 (1C).

4'-pentylphenol (3c)

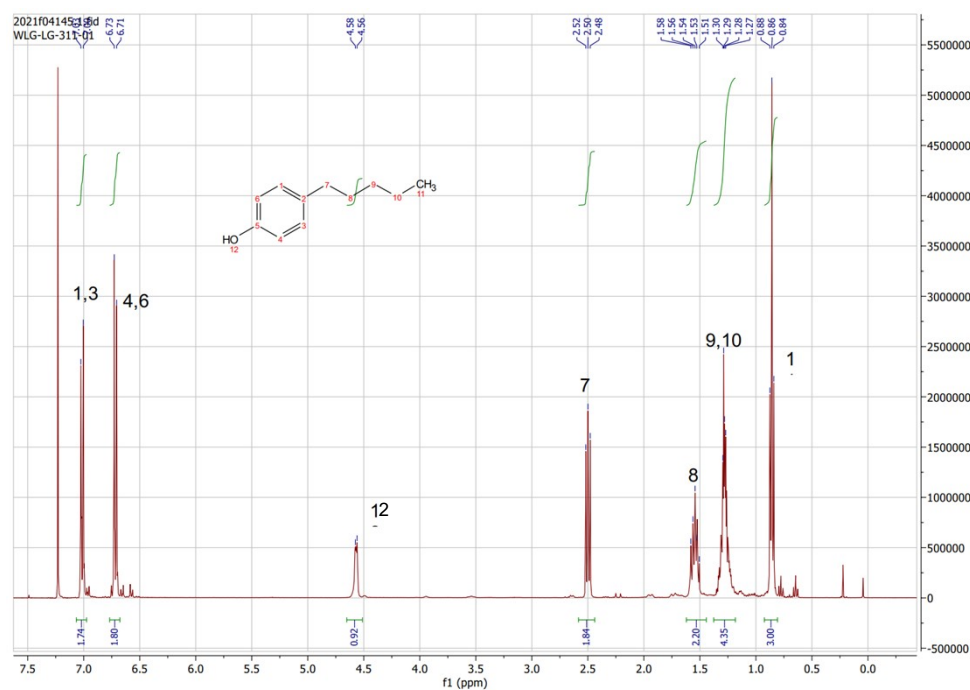


Figure S11: ¹H NMR of 4'-pentylphenol.

¹H NMR (400 MHz, Chloroform-*d*) δ (ppm) = 7.01 (d, J = 8.5 Hz, 2H), 6.72 (d, J = 8.5 Hz, 2H), 4.57 (d, J = 6.2 Hz, 1H), 2.52 – 2.48 (t, 2H), 1.58 – 1.51 (dt, J = 15.1, 8.2 Hz, 2H), 1.28 (dd, J = 6.7, 3.6 Hz, 4H), 0.86 (t, J = 6.9 Hz, 3H).

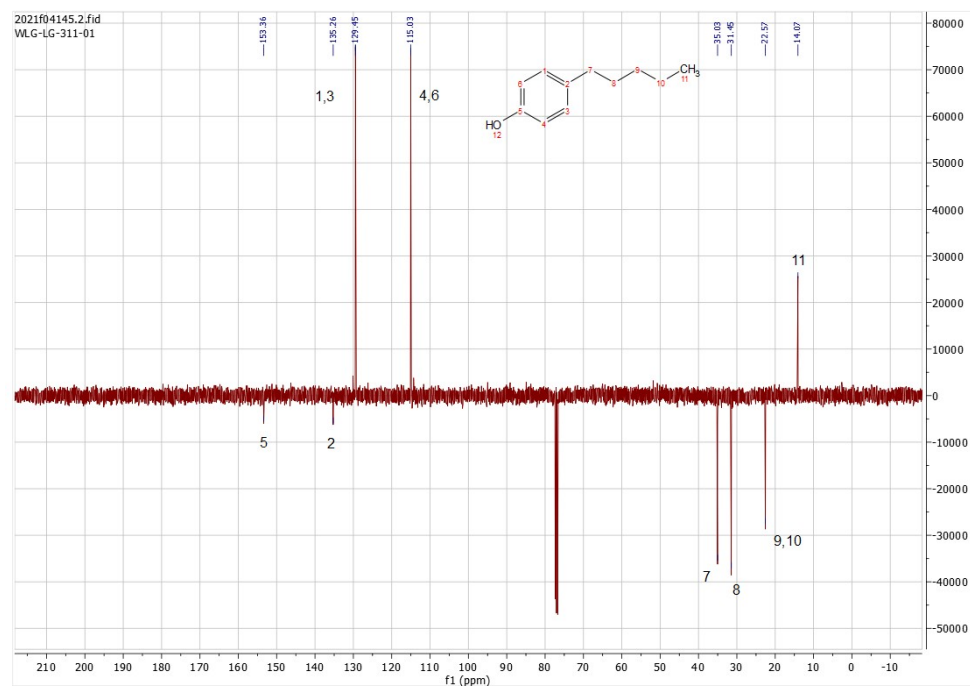


Figure S12: ¹³C NMR of 4'-pentylphenol.

¹³C (APT) NMR (100 MHz, Chloroform-*d*) δ (ppm) = 153.36 (1C), 135.26 (1C), 129.26 (2C), 115.03 (2C), 35.03 (1C), 31.45 (1C), 22.57 (2C), 14.07 (1C).

4'-hexylphenol (4c)

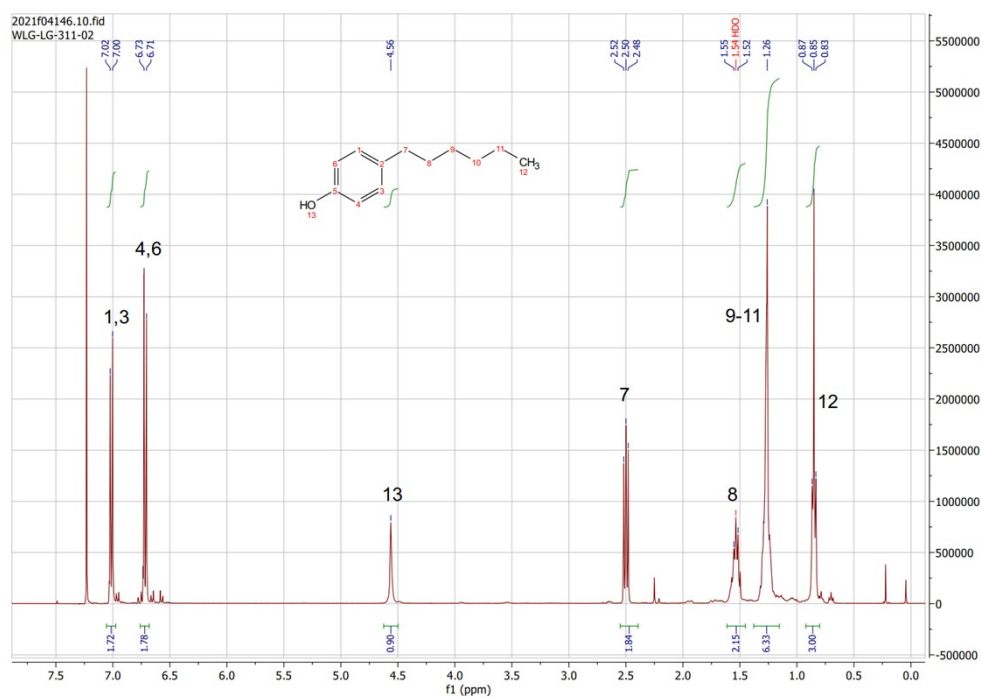


Figure S13: ¹H NMR of 4'-hexylphenol.

¹H NMR (400 MHz, Chloroform-*d*) δ (ppm) = 7.01 (d, J = 8.6 Hz, 2H), 6.72 (d, J = 8.5 Hz, 2H), 4.56 (s, 1H), 2.52 – 2.48(t, 2H), 1.53 (d, J = 14.7 Hz, 2H), 1.26 (s, 6H), 0.87 – 0.83 (m, 3H).

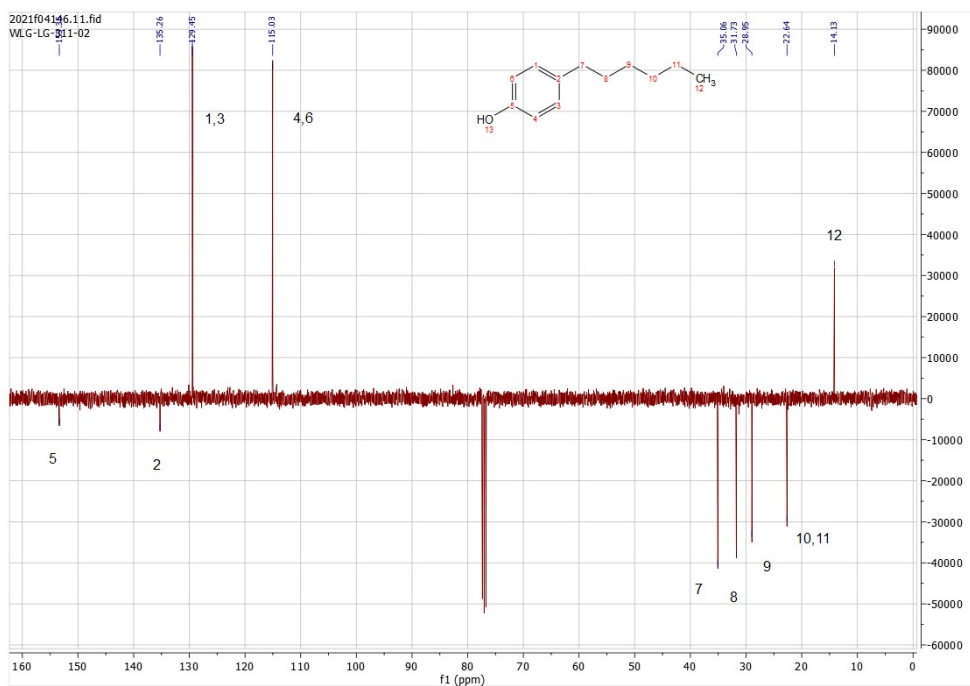


Figure S14: ¹³C NMR of 4'-hexylphenol.

¹³C (APT) NMR (100 MHz, Chloroform-*d*) δ (ppm) = 153.35 (1C), 135.26 (1C), 129.45 (2C), 115.03 (2C), 35.06(1C), 31.73 (1C), 28.95 (1C), 22.64 (2C), 14.13 (1C).

4'-heptylphenol (5c)

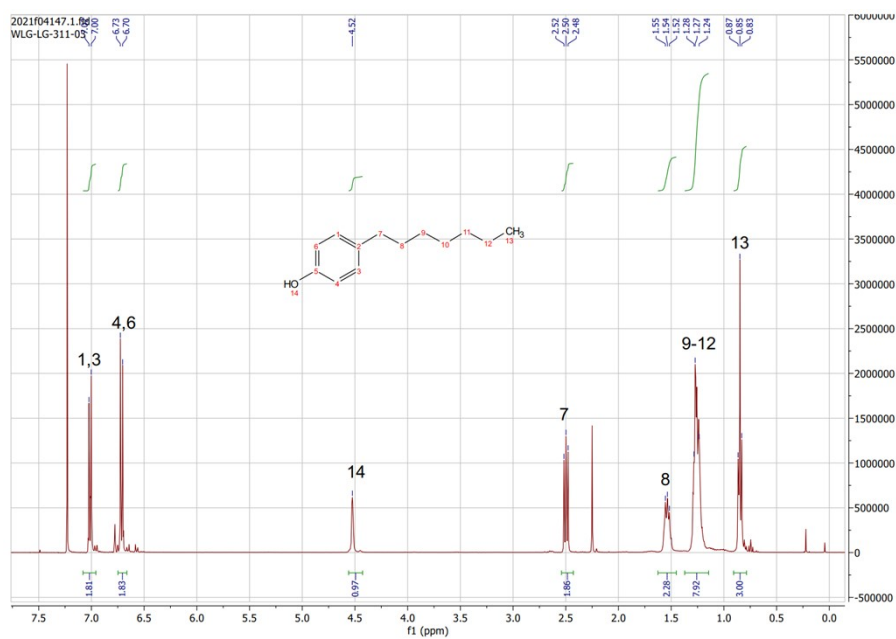


Figure S15: ^1H NMR of 4'-heptylphenol.

^1H NMR (400 MHz, Chloroform- d) δ (ppm) = 7.01 (d, J = 8.5 Hz, 2H), 6.71 (d, J = 8.5 Hz, 2H), 4.52 (s, 1H), 2.52 – 2.48 (t, 2H), 1.55 – 1.52 (m, 2H), 1.28 – 1.24 (m, 8H), 0.87 – 0.83 (m, 3H).

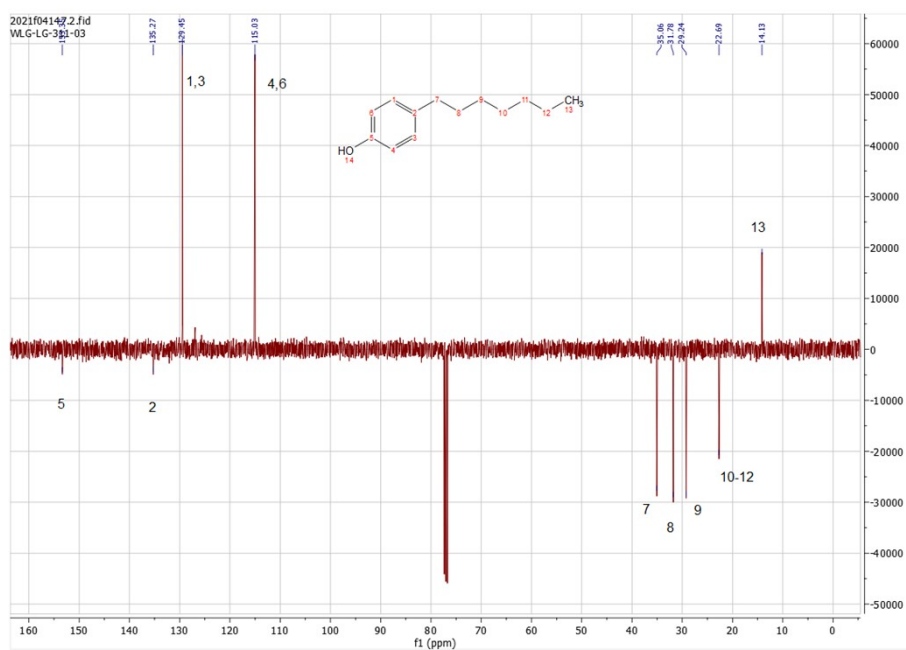


Figure S16: ^{13}C NMR of 4'-heptylphenol.

^{13}C (APT) NMR (100 MHz, Chloroform- d) δ (ppm) = 153.35 (1C), 135.27 (1C), 129.45 (2C), 115.03 (2C), 35.06 (1C), 31.78 (1C), 29.21 (1C), 22.69 (3C), 14.13 (1C).

4'-nonylphenol (7c)

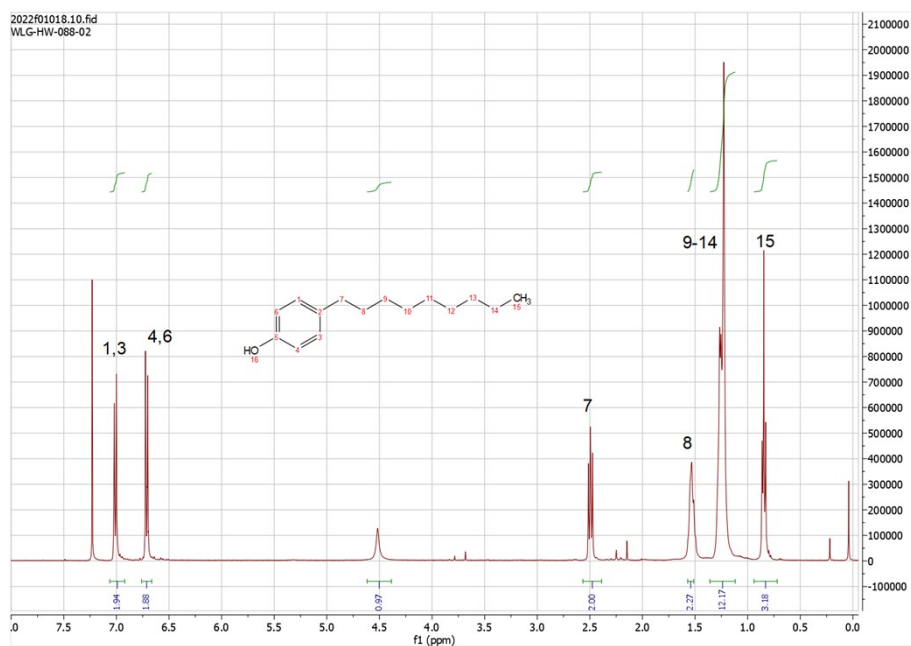


Figure S17: ^1H NMR of 4'-nonylphenol.

^1H NMR (400 MHz, Chloroform- d) δ (ppm) = 7.06 – 6.92 (m, 2H), 6.76 – 6.66 (m, 2H), 4.52 (s, 1H), 2.57 – 2.39 (m, 2H), 1.54 (d, J = 5.7 Hz, 2H), 1.36 – 1.12 (m, 12H), 0.85 (t, J = 6.7 Hz, 3H).

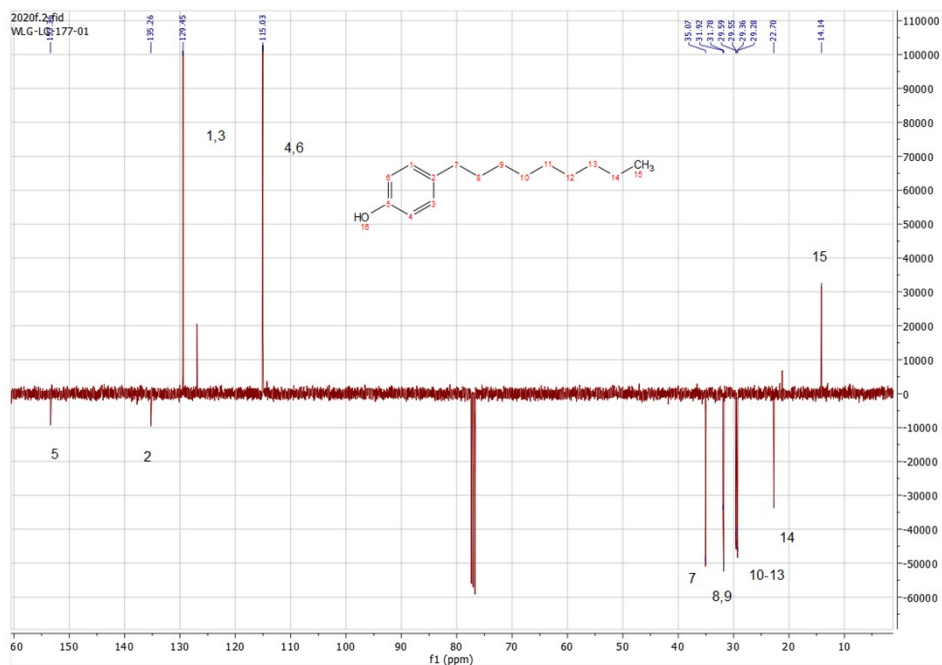


Figure S18: ^{13}C NMR of 4'-nonylphenol.

^{13}C (APT) NMR (100 MHz, Chloroform- d) δ (ppm) = 153.36 (1C), 135.26 (1C), 129.45 (2C), 115.03 (2C), 35.07 (1C), 31.92 (1C), 31.78 (1C), 29.59 (1C), 29.55 (1C), 29.36 (1C), 29.28 (1C), 14.14 (1C).

4'-ethyl-*N,N*-dimethylaniline (18c)

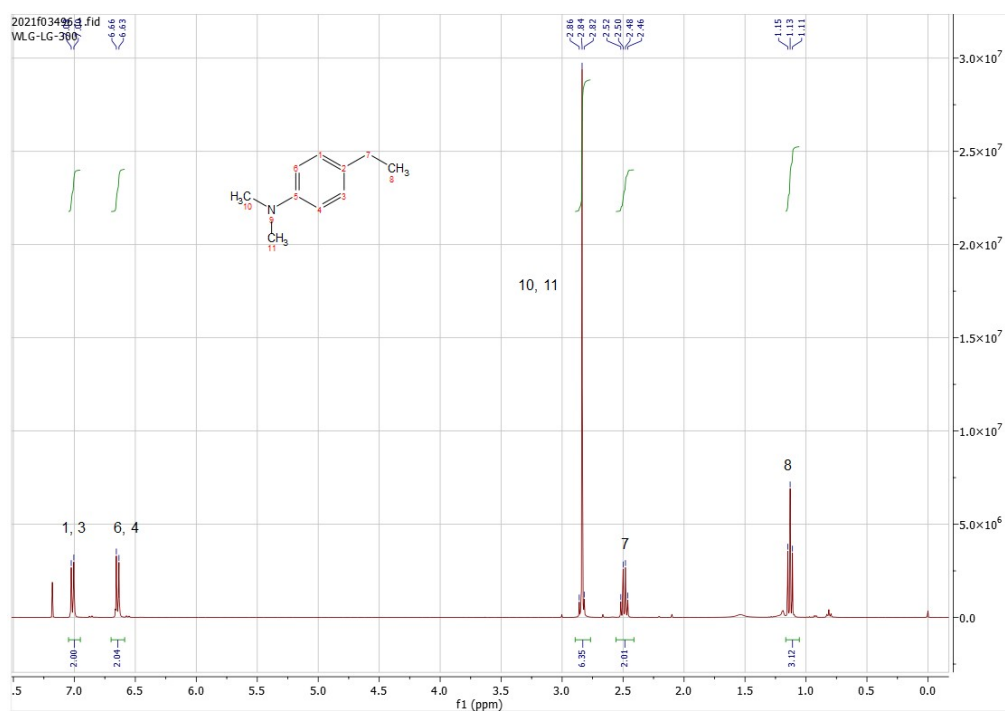


Figure S19: ^1H NMR of 4'-ethyl-*N,N*-dimethylaniline.

^1H NMR (400 MHz, Chloroform-*d*) δ (ppm) = 7.01 (d, J = 8.6 Hz, 2H), 6.64 (d, J = 8.6 Hz, 2H), 2.84 (s, 6H), 2.49 (q, J = 7.6 Hz, 2H), 1.13 (t, J = 7.6 Hz, 3H).

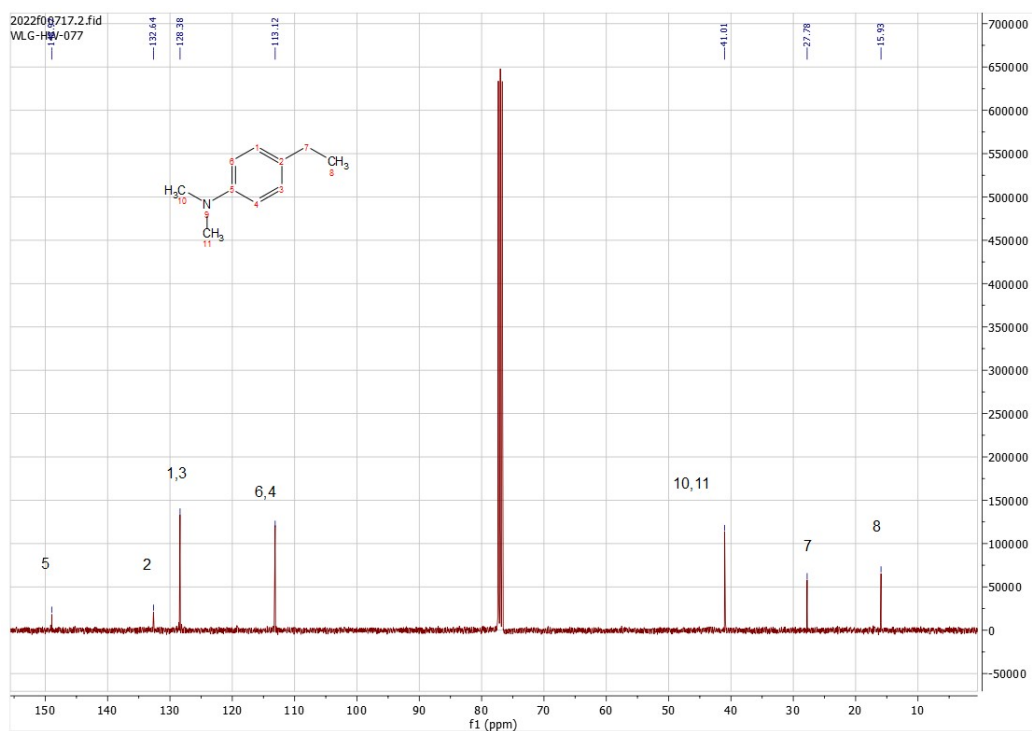


Figure S20: ^{13}C NMR 4'-ethyl-*N,N*-dimethylaniline.

$^{13}\text{C}\{^1\text{H}\}$ NMR (100 MHz, Chloroform-*d*) δ (ppm) = 148.79 (1C), 132.64 (1C), 128.38 (2C), 113.12 (2C), 41.01 (2C), 27.78 (1C), 15.93 (1C).

4'-propylaniline (9c)

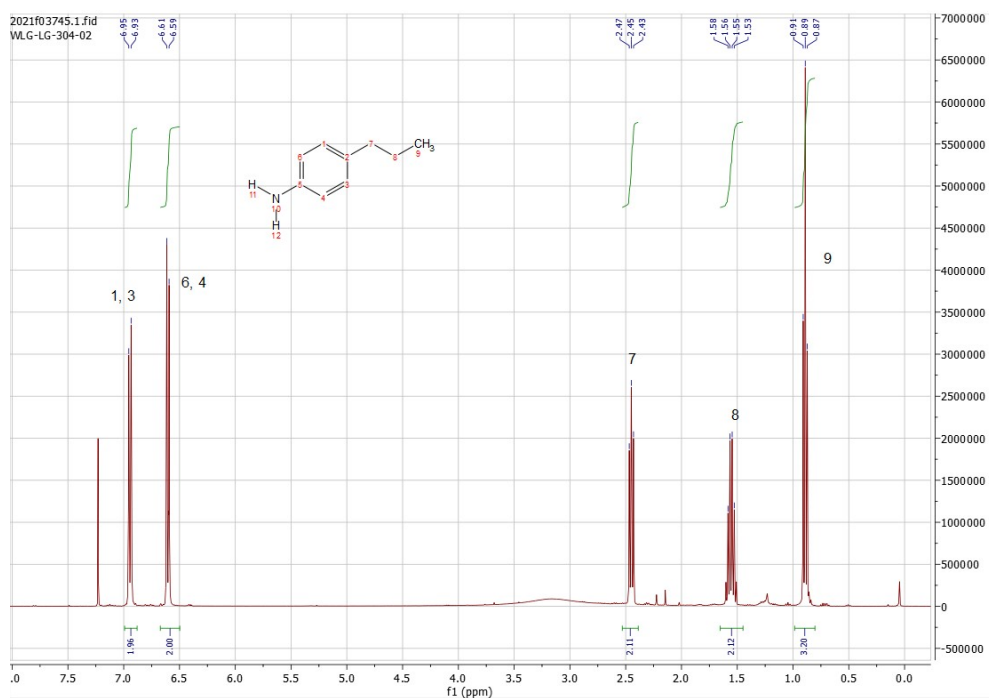


Figure S21: ^1H NMR of 4'-propylaniline.

^1H NMR (400 MHz, Chloroform-*d*) δ (ppm) = 6.94 (d, J = 8.2 Hz, 2H), 6.60 (d, J = 8.4 Hz, 2H), 2.53 – 2.39 (m, 2H), 1.56 (q, J = 7.4 Hz, 2H), 0.89 (t, J = 7.3 Hz, 3H).

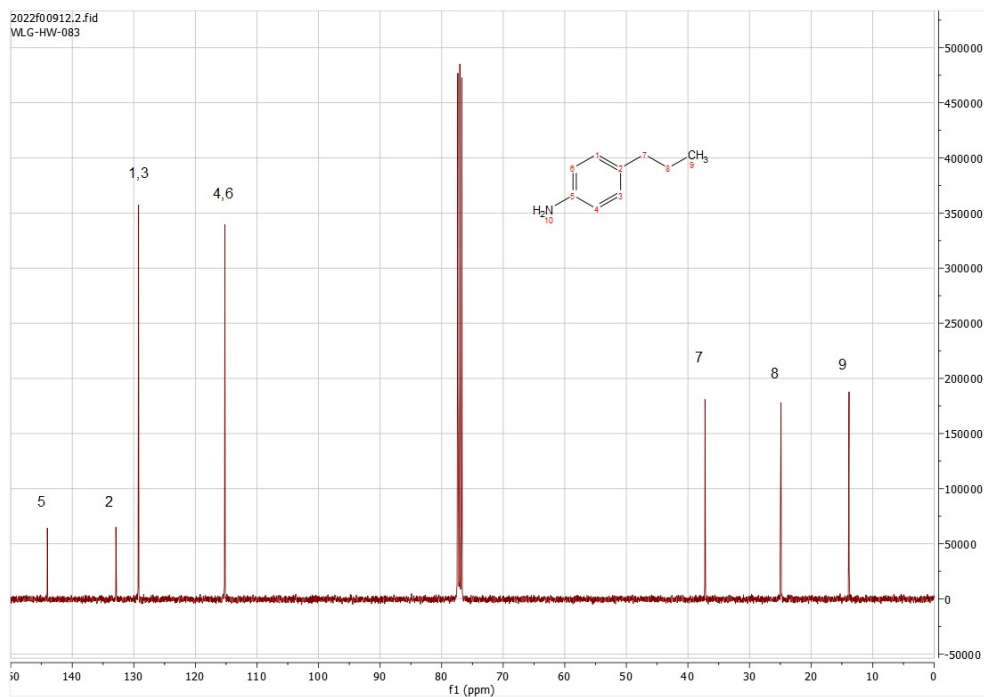


Figure S22: ^{13}C NMR of 4'-propylaniline.

$^{13}\text{C}\{^1\text{H}\}$ NMR (100 MHz, Chloroform-*d*) δ (ppm) = 144.05 (1C), 132.91 (1C), 129.22 (2C), 115.21 (2C), 37.22 (1C), 24.88 (1C), 13.83 (1C).

4-amino-2-ethylphenol (11c)

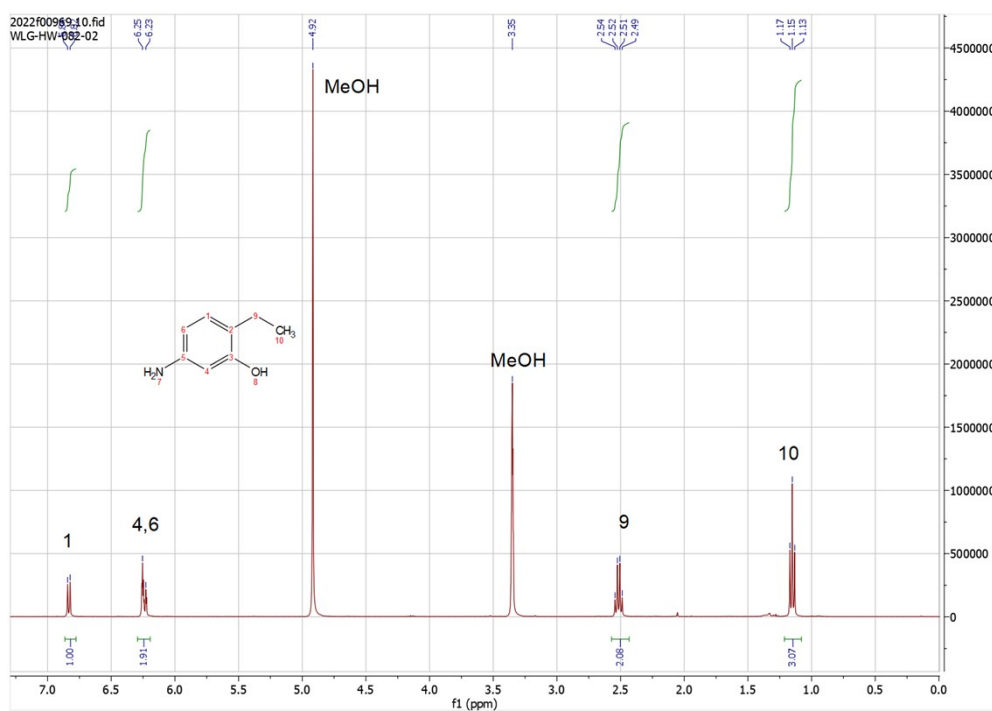


Figure S23: ^1H NMR of 5-amino-2-ethylphenol.

^1H NMR (400 MHz, Methanol- d_4) δ (ppm) = 6.83 (d, J = 7.8 Hz, 1H), 6.24 (d, J = 10.5 Hz, 2H), 2.52 (q, J = 7.5 Hz, 2H), 1.15 (t, J = 7.5 Hz, 3H).

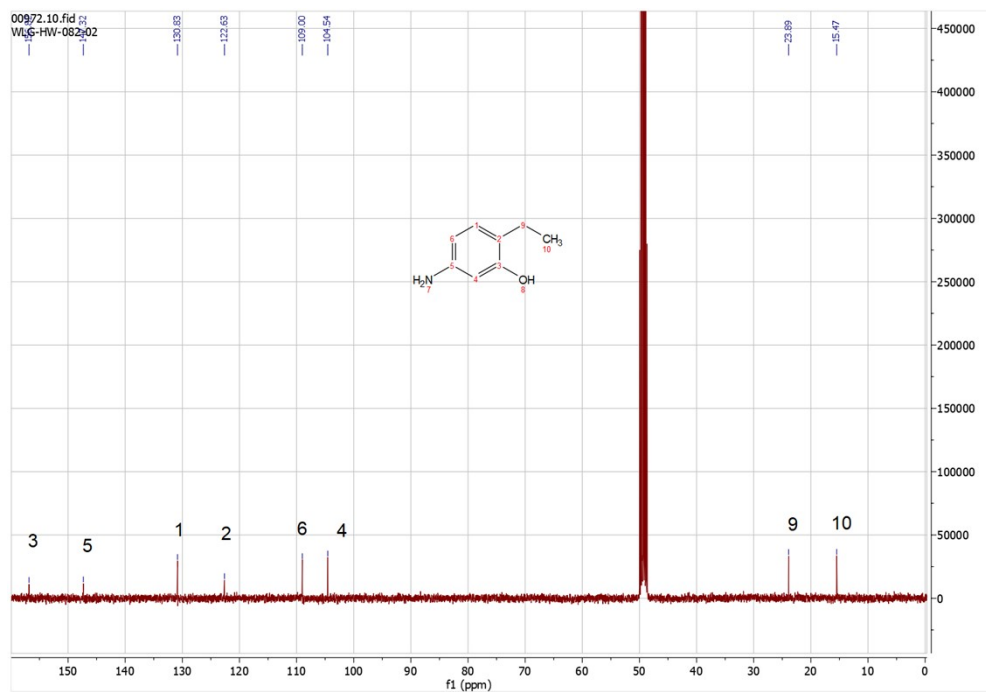


Figure S24: ^{13}C NMR of 5-amino-2-ethylphenol.

$^{13}\text{C}\{^1\text{H}\}$ NMR (100 MHz, Methanol- d_4) δ (ppm) = 156.82 (1C), 147.32 (1C), 130.83 (1C), 122.63 (1C), 109.00 (1C), 104.54 (1C), 23.89 (1C), 15.47 (1C).

4'-ethyl-3'-methylaniline (15c)

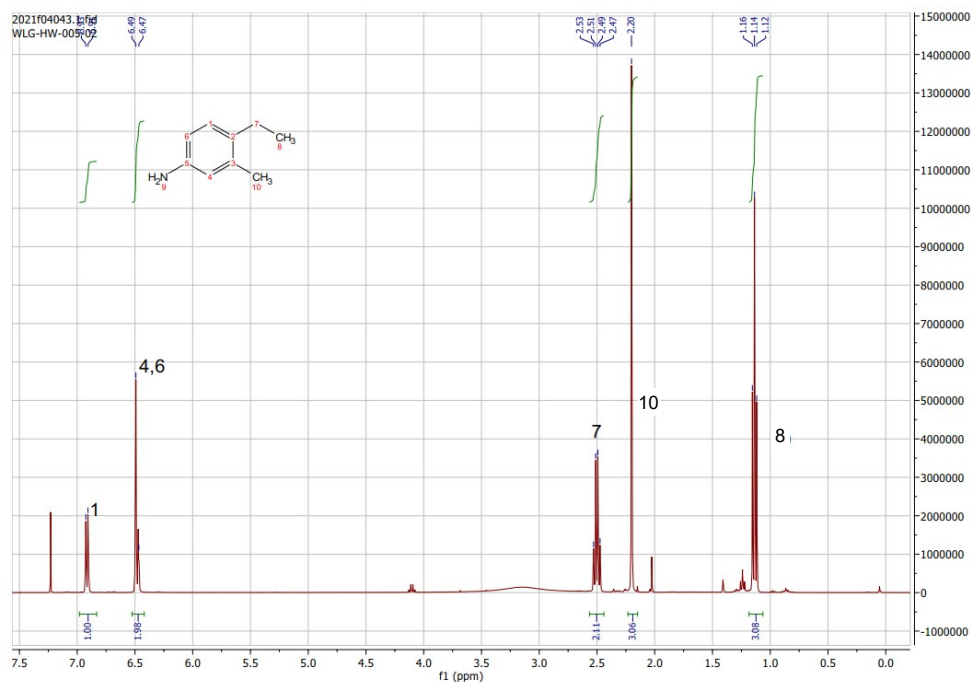


Figure S25: ^1H NMR of 4'-ethyl-3'-methylaniline.

^1H NMR (400 MHz, Chloroform-*d*) δ (ppm) = 6.92 (d, J = 7.7 Hz, 1H), 6.48 (d (J = 10.3 Hz) and s, 2H), 2.50 (q, J = 7.5 Hz, 2H), 2.20 (s, 3H), 1.14 (t, J = 7.5 Hz, 3H).

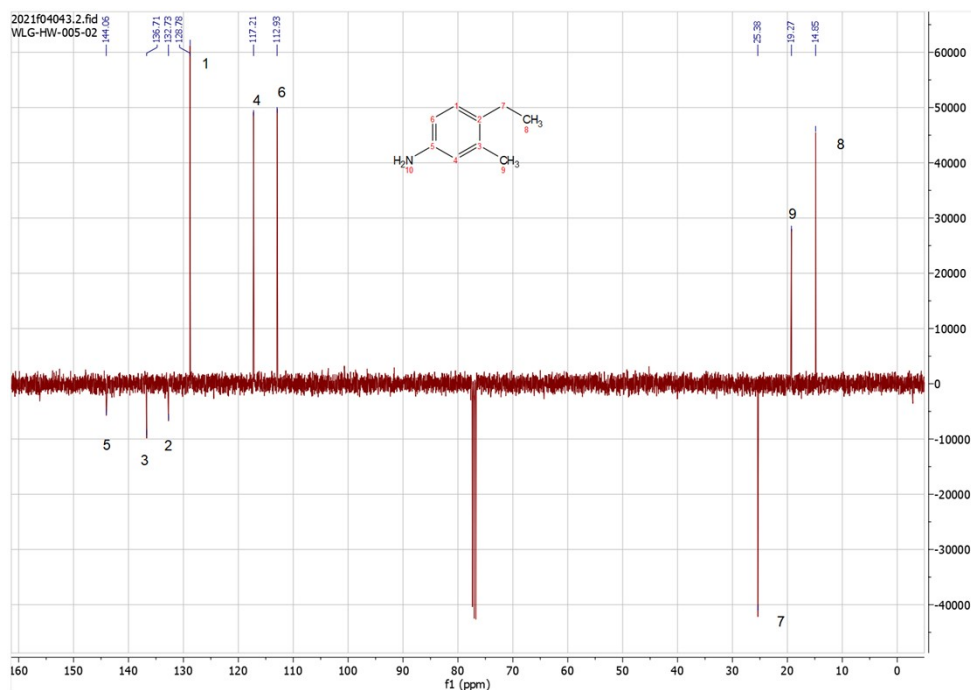


Figure S26: ^{13}C NMR of 4'-ethyl-3'-methylaniline.

^{13}C (APT) NMR (100 MHz, Chloroform-*d*) δ (ppm) = 144.06 (1C), 136.71 (1C), 132.73 (1C), 128.78 (1C), 117.21 (1C), 112.93 (1C), 25.38 (1C), 19.27 (1C), 14.85 (1C).

***N,N*,4-triethylaniline (19c)**

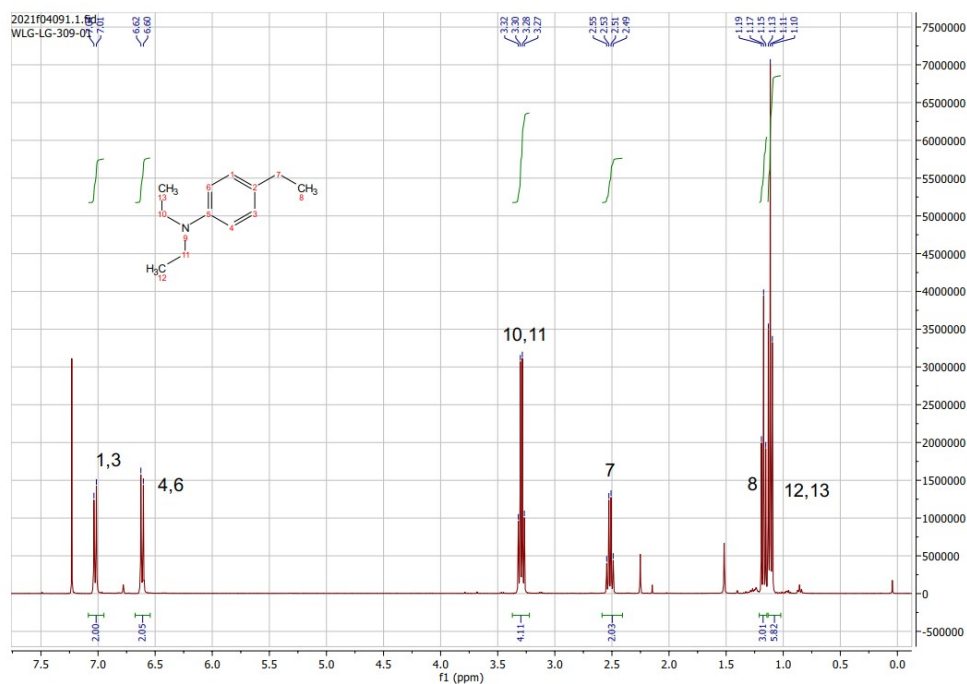


Figure 27: ^1H NMR of *N,N*,4-triethylaniline.

^1H NMR (400 MHz, Chloroform-*d*) δ (ppm) = 7.03 (d, J = 8.7 Hz, 2H), 6.61 (d, J = 8.7 Hz, 2H), 3.29 (q, J = 7.1 Hz, 4H), 2.52 (q, J = 7.6 Hz, 2H), 1.17 (t, J = 7.6 Hz, 3H), 1.11 (t, J = 7.1 Hz, 6H).

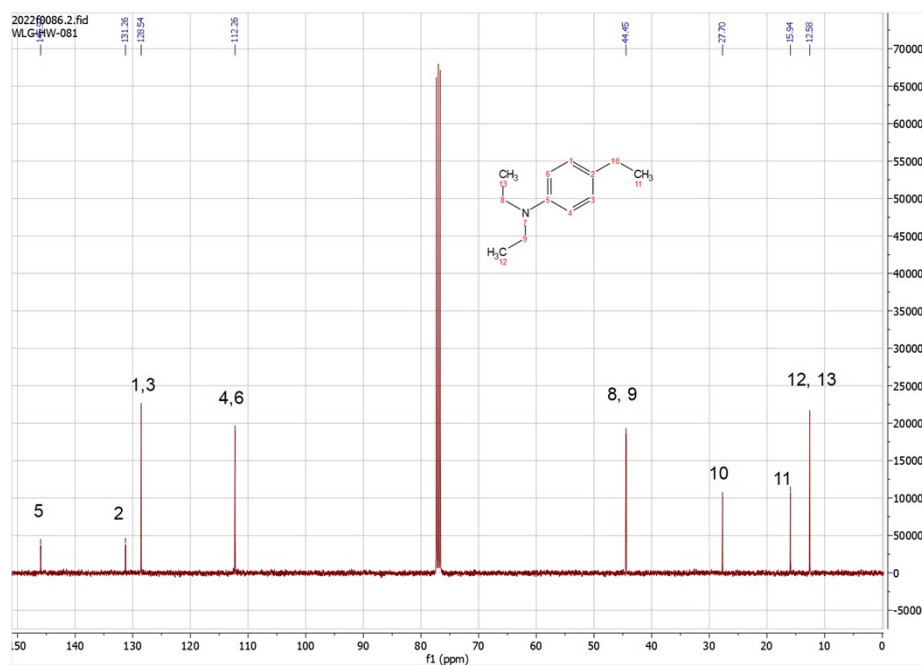


Figure 28: ^{13}C NMR of *N,N*,4-triethylaniline.

$^{13}\text{C}\{^1\text{H}\}$ NMR (100 MHz, Chloroform-*d*) δ (ppm) = 145.97 (1C), 131.26 (1C), 128.54 (1C), 112.26 (1C), 44.45 (2C), 27.70 (1C), 15.94 (1C), 12.58 (2C).

References

- 1 J. Ruiz-Caro, A. Basavapathruni, J. T. Kim, C. M. Baily, L. Wang, K. S. Anderson, A.D. Hamilton and W. L. Jorgensen, *Bioorg. Med. Chem. Lett.*, 2006, **16**, 688.
- 2 (a) WO 2004/056782 A1, PTC int. Appl. 2004; (b) C. Schultze and B. Schmidt, *J. Org. Chem.*, 2018, **83**, 5210; (c) Y. Hu, Y. Yang, Y. Yu, G. Wen, N. Shang, W. Zhuang, D. Lu, B. Zhou, B. Liang, X.Yue, F. Li, J. Du and X. Bu, *J. Med. Chem.*, 2013, **56**, 6033.
- 3 H. Fiege, H.-W. Voges, T. Hamamoto, S. Umemura, T. Iwata, H. Miki, Y. Fujita, H.-J. Buysch, D. Garbe and W. Paulus, 2002, "Phenol Derivatives". Ullmann's Encyclopedia of Industrial Chemistry. Weinheim: Wiley-VCH.
- 4 R. Murashige, Y. Hayashi, S. Ohmori, A. Torii, Y. Aizu, Y. Muto, Y. Murai, Y. Oda and M. Hashimoto, *Tetrahedron*, 2011, **67**, 641.
- 5 K. L. Luska, A. Bordet, S. Tricard, I. Sinev, W. Grünert, B. Chaudret and W. Leiter, *ACS Catal.*, 2016, **6**, 3719